Computers and Mathematics with Applications 64 (2012) 709–720

Contents lists available at SciVerse ScienceDirect

Computers and Mathematics with Applications

journal homepage: www.elsevier.com/locate/camwa

Design and implementation of fuzzy sliding mode controllers for generalized projective synchronization of chaos horizontal platform systems

Neng-Sheng Pai *, Shih-Ping Chang

Department of Electrical Engineering, National Chin-Yi University of Technology, Taichung, Taiwan

ARTICLE INFO

Keywords:
Fuzzy sliding mode control
Horizontal platform vibration system
Chaos system
Lyapunov stability theorem

ABSTRACT

This paper presents robust chattering-free fuzzy sliding mode control (FSMC) as a way to achieve generalized projective synchronization (GPS) of two horizontal chaos platform vibration systems with system uncertainty and external disturbance. An appropriate sliding surface is acquired through an SMC design such that the error state trajectories of a master–slave system will reach such a sliding surface and approaches to the origin. Based on the Lyapunov stability theory, we address the design schemes of integration fuzzy sliding mode control, where the reaching law is proposed by a set of linguistic rules and the control input is chattering free. As a consequence, the system is simulated and experimented to demonstrate that the error state tends to be stabilized and the chattering problem can be thus resolved, implying that the slave horizontal platform system (HPS) is GPS with the master HPS.

© 2011 Elsevier Ltd. All rights reserved.

1. Introduction

Having been well discussed, Chaos can be found in a wide variety of research fields, e.g. electrical engineering, electronics, communication, biology, mathematics, physics, chemistry, economics, etc. There is the Lorenz system [1] on the subject of atmospheric science, Duffing system [2] on mechanics, Rössler system [3] on chemical engineering, and Chua's circuit [4] on circuitry.

In 2003, a linear feedback master–slave horizontal platform vibration system is simulated to validate that two chaos systems, with distinct initial values, can be synchronized through a state error feedback control by Ge et al. [5]. Subsequently, Wu et al. [6,7] made a contribution to the robust control design in order to inhibit chaos. In 2007, Ma Mihua et al. [8] explored the effect of various system parameters on the robust synchronization error. It takes a long period of time and cost a large amount of money to watch the chaos posed when a mechanical system is operated with potential malfunction. In consideration of cost cut and prospective application, the mechanical system is thus replaced with electronics in the same dynamic conditions.

Over the years, the analysis and application of a chaos system has received much attention from a great number of researchers. The demonstration and control of chaos systems thus becomes an issue of significance in such fields. In 1989, Ott, Grebogi, and Yorke first proposed a method of their own, abbreviated as O.G.Y chaos control method [9]. Subsequent to the work, proposed by Pecora and Carroll [10], that two independent systems are synchronized so as to solve the chaos problem, an increasing number of researchers develop methods on their own to reach synchronization in various approaches such as adaptive control, feedback control, sliding mode control, fuzzy sliding mode control, and so on [11–18]. Amongst all

* Corresponding author. Fax: +886 4 23924419.
E-mail addresses: pai@mail.ncut.edu.tw, pai@ncut.edu.tw (N.-S. Pai).

0898-1221/$ – see front matter © 2011 Elsevier Ltd. All rights reserved.
doi:10.1016/j.camwa.2011.10.037

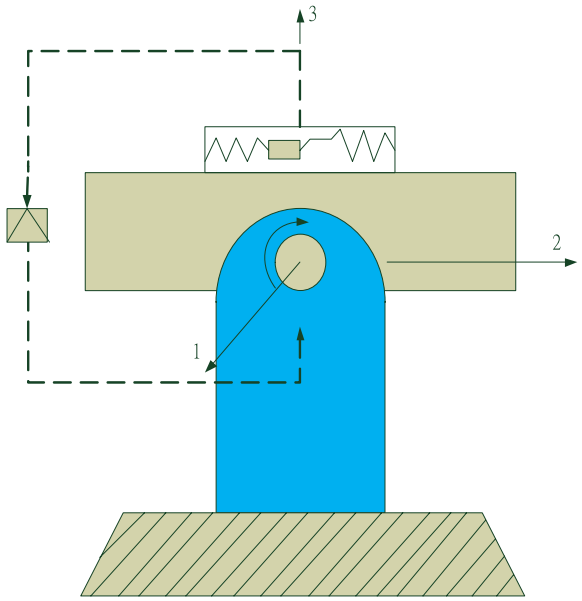

Fig. 1. Horizontal platform system.

kinds of chaos synchronization, projective synchronization, characterized by a scaling factor that two systems synchronize proportionally, is one of the most interesting problems. This type of chaos synchronization was first reported by Mainieri and Rehacek [19], where they declared that the two identical systems (master and slave) could be synchronized up to a scaling factor α. They further stated that the scaling factor was dependent on the chaotic evolution and initial conditions so that the ultimate state of projective synchronization was unpredictable. However, in early work on projective synchronization, the investigated chaotic systems must be partially linear. Later, some authors extended it to a general class of chaotic systems without the limitation of partial-linearity (i.e., non-partially-linear systems). Because it is associated with projective synchronization and generalized one, they called it "generalized projective synchronization" (GPS). In the present paper, we focus on the generalized projective synchronization between two HPS via sliding mode control.

The furious chattering remains the problem of the greatest significance in the sliding mode control, featuring the invariance. Conventionally, chattering is removed in a manner that approximates the discontinuous control as a continuous case or degrades the precision required on the sliding surface, at the cost of invariance featured. Essentially, the chattering cannot be removed by the roots. On the other hand, the robustness, caused by invariance, exists only when the system is operated in sliding mode. This paper is presented with a focus on the design of a fuzzy sliding mode controller, which is achieved by the system dynamic locus approaching the sliding surface. The dramatic chattering can be thus removed in such an effective way that a high degree of robustness as well as stability can be preserved [20,21].

The rest of the paper is organized as follows. Section 2 describes dynamic model of the horizontal platform systems and implemented using OP integrated circuits. In Section 3, the fuzzy sliding mode controller for the GPS is developed and the criteria for the system stability scheme are proven. Next, simulations are performed and experimental results are given to verify the effectiveness of the proposed control scheme in Section 4. Finally, the conclusions are drawn in Section 5.

2. HPS description and circuit implementation

Illustrated in Figs. 1 and 2 are the nonlinear configuration of a horizontal platform system (HPS) [5]. The system is free to revolve about the horizontal axis, with an accelerator located at the left side of the platform. As soon as the platform deviates from the horizon, a signal is transmitted by the accelerator to generate a reverse torque to keep the platform balanced. The dynamic equation of HPS [5] is expressed as

$$A\ddot{x}(t) + D\dot{x}(t) + rg \sin x(t) - \frac{3g}{R}(B - C)\cos x(t) \cdot \sin x(t) = F \cos \omega t \tag{1}$$

where A, B and C represent the rotational inertia of the platform rotation axis, as illustrated in Fig. 2, D is the damping coefficient, R the earth radius, r the proportional constant of the accelerator, and g the gravitational constant. Besides, x denotes the rotation angle of the platform measured relative to the earth, $F \cos \omega t$ the harmonic torque, and $x_1(t) = x(t)$

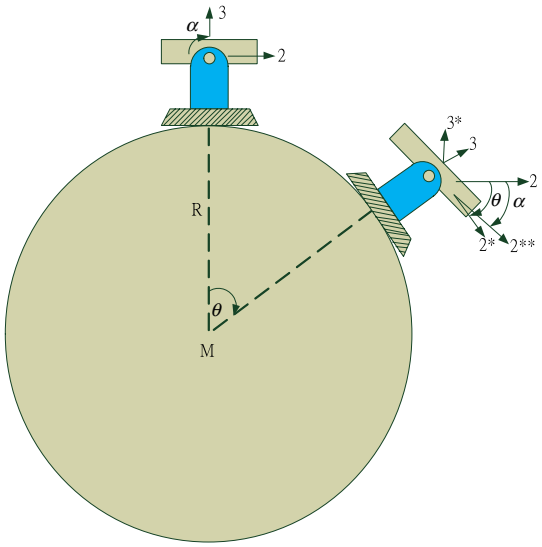

Fig. 2. Horizontal platform system on the earth.

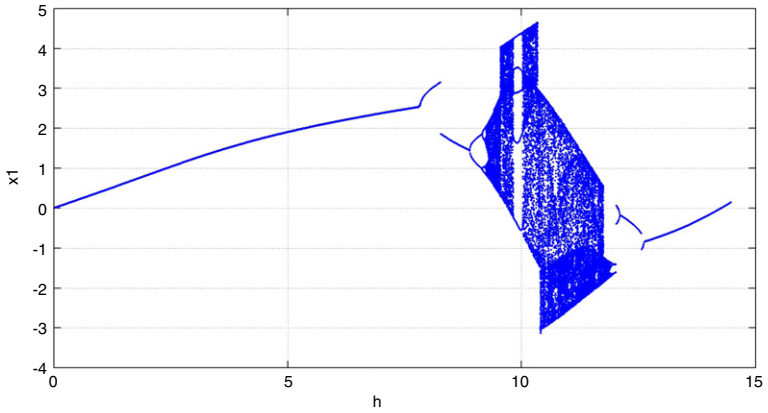

Fig. 3. Bifurcation diagrams of parameter h versus system state x_1.

together with $x_2(t) = \dot{x}(t)$ the system state variables. For simplicity, the system parameters are rewritten as $a = D$, $rg = b$, $l = \frac{3g}{R}(B - C)$ and $F = h$. With the above mentioned parameters, the HPS state equation [5] is expressed as

$$\begin{aligned} \dot{x}_1 &= x_2 \\ \dot{x}_2 &= -ax_2 - b\sin x_1 + l\cos x_1 \cdot \sin x_1 + h\cos \omega t. \end{aligned} \tag{2}$$

This HPS (2) exhibits complex dynamics and has been studied by Ge et al. [5] for values of h in the range $0 < h < 15$ and constant values of $a = 4/3$, $b = 3.776$, $l = 4.6 \times 10^{-6}$, $\omega = 1.8$. Fig. 3 shows the bifurcation diagram. In this case, the qualitative behavior of the system is shown against a varying parameter h from 0 to 15. As parameter h is increased from zero, periodic motion exists around one of the center points, including T-, $2T$-, $4T$- and multi-periodic motions. However, at $h = 9.3$, the multi-periodic motion is replaced by irregular motion. Fig. 4 illustrates the irregular motion exhibited by this system for $h = 34/3$, and with initial condition of $(x_1, x_2) = (0, 0)$. Fig. 5 reveals that the corresponding maximum Lyapunov exponent of HPS versus parameter h in the range of $(0, 15)$. It can be seen that a positive maximum Lyapunov exponent does exist in the range $9.3 < h < 11.8$, and thus it can be inferred that the HPS trajectory will be in a state of chaotic motion in this range.

Due to a high cost required in the mechanic hardware implementation, the platform system as represented in Eq. (2) is realized by a circuit, mainly made up of OP amplifiers, and simulated by ORCAD shown in Fig. 6. With the entity photo of hardware system shown in Fig. 7, the simulation is in good agreement with the experimental results shown in Fig. 8. For the purpose of validating the chaos in the hardware system implemented, the data acquired is verified by a Lyapunov exponent examination. Illustrated in Fig. 9 is a positive value of the Lyapunov exponent, a sign of chaos oscillation [22]. In the next section, the FSMC control scheme will be used to achieve the generalized projective synchronization problem of a master–slave (drive-response) horizontal platform systems.

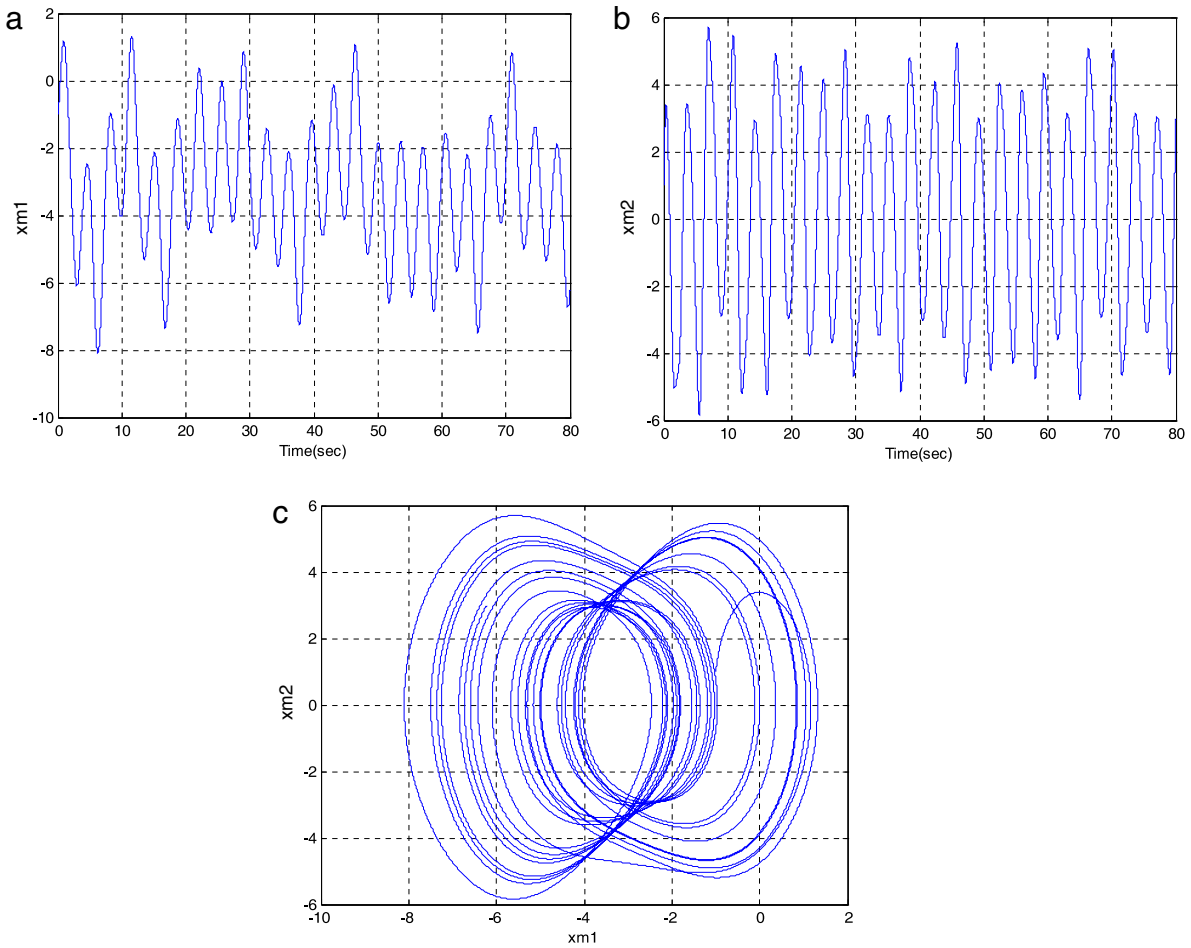

Fig. 4. The time responses of system (a) x_1 state; (b) x_2 state, and the phase plane trajectory of x_1 versus x_2.

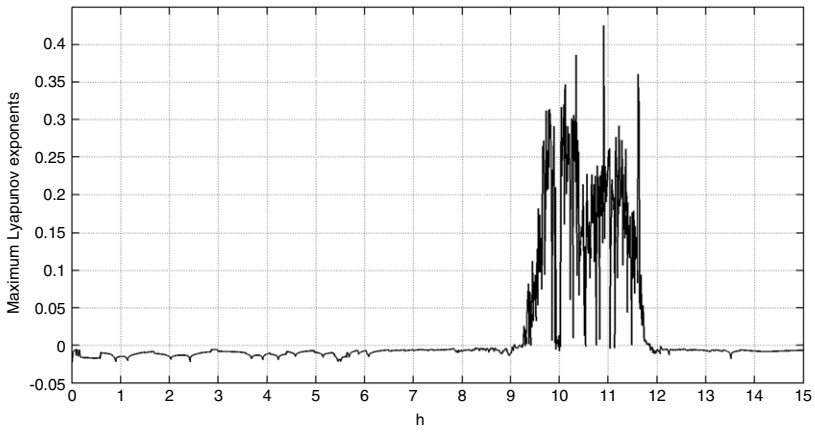

Fig. 5. The maximum Lyapunov exponents of HPS plotted as a function of the parameter h. (The positive Lyapunov exponents exist in $9.3 < h < 11.8$).

3. Generalized projective synchronization for the HPS via FSMC

In a substantial system, it is very unlikely to exclude the external disturbance completely. Due to inadequate system information and over simplification in the system modeled, there occurs system uncertainty; an issue needed to be addressed in this paper.

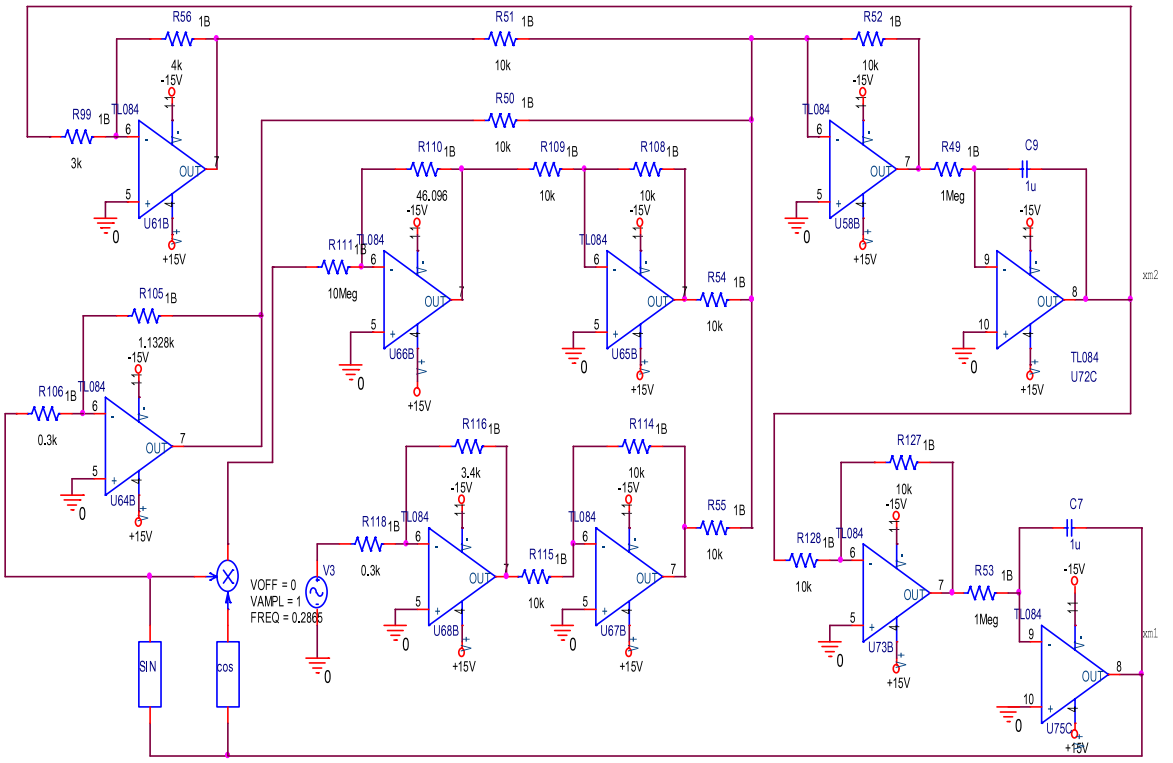

Fig. 6. Simulation circuit diagram of HPS implemented in ORCAD.

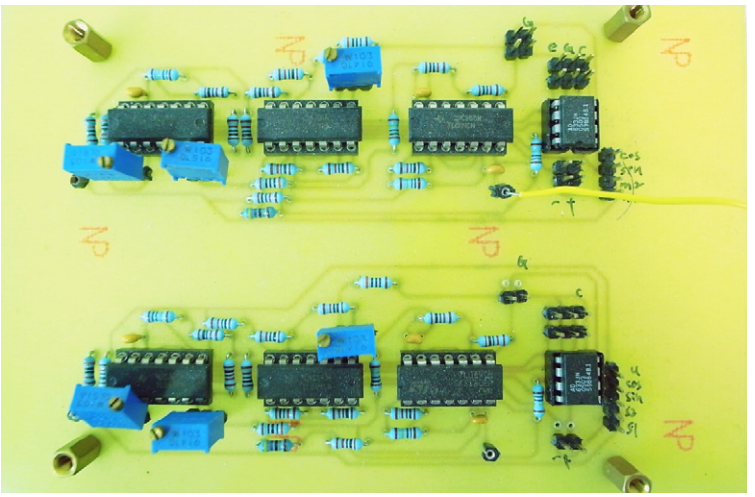

Fig. 7. Photo of the HPS circuit module.

The master–slave equation in a horizontal platform system is represented as

$$\text{Master: } \begin{cases} \dot{x}_{m1} = x_{m2} \\ \dot{x}_{m2} = -ax_{m2} - b\sin x_{m1} + l\cos x_{m1} \cdot \sin x_{m1} + h\cos \omega t \end{cases} \tag{3}$$

$$\text{Slave: } \begin{cases} \dot{x}_{s1} = x_{s2} \\ \dot{x}_{s2} = -ax_{s2} - b\sin x_{s1} + l\cos x_{s1} \cdot \sin x_{s1} + h\cos \omega t + u + \Delta\xi + d\,(t) \end{cases} \tag{4}$$

where u represents the input to the controller, $\Delta\xi$ the system uncertainty, and $d\,(t) = 0.1\cos\,(t)$ the external disturbance with parameters $a = 4/3$, $b = 3.776$, $l = 4.6 \times 10^{-6}$, $h = 34/3$, $\omega = 1.8$, and $\Delta\zeta = 0.1\sin\,(t)$. Generalized projective

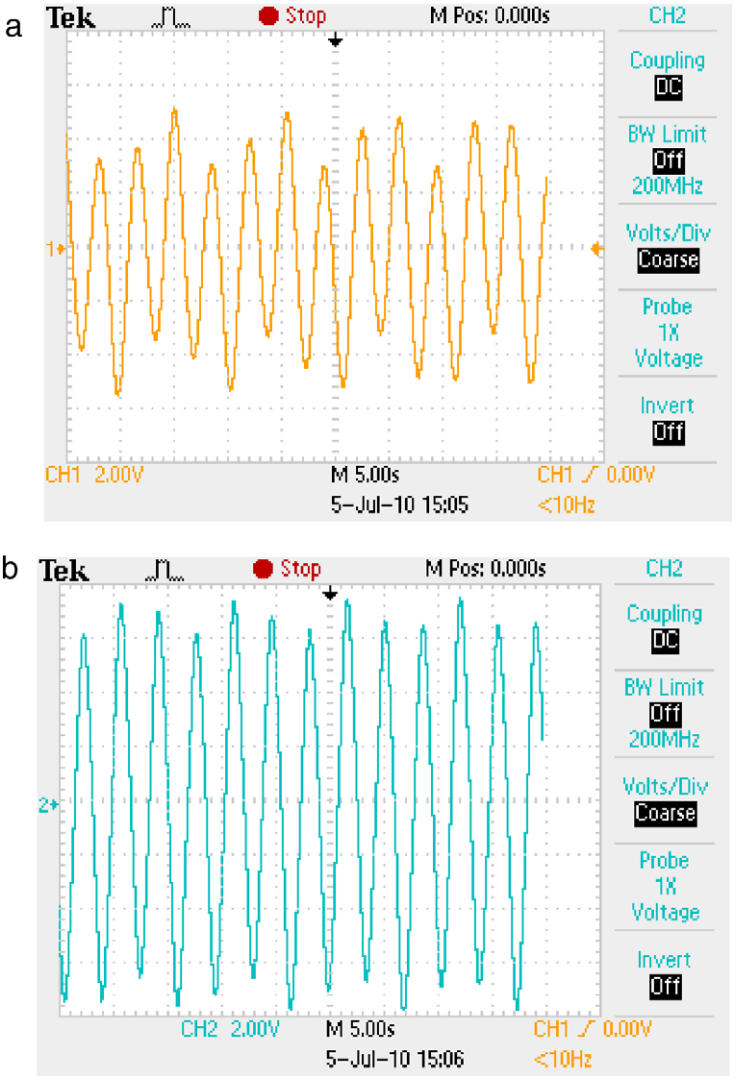

Fig. 8. Actual system responses with hardware (a) x_1 state; (b) x_2 state.

synchronization (GPS) is aimed to achieve

$$\lim_{t\to\infty} \|x_s(t) - \rho x_m(t)\| = 0 \tag{5}$$

where $\alpha \neq 0$ is a constant scaling factor and $\|\cdot\|$ is the Euclidean norm of a vector, then the GPS of Eqs. (3) and (4) is achieved.

Remark 1. Note that identical synchronization and anti-synchronization are special cases of GPS with $\alpha = 1$ and $\alpha = -1$, respectively.

Derived from Eqs. (3) to (4), the error state equation is expressed as

$$\begin{aligned} e_1 &= x_{s1} - \rho x_{m1} \\ e_2 &= x_{s2} - \rho x_{m2} \end{aligned} \tag{6}$$

It then follows from Eq. (6) that

$$\begin{aligned} \dot{e}_1 &= \dot{x}_{s1} - \rho\dot{x}_{m1} = x_{s2} - \rho x_{m2} = e_2 \\ \dot{e}_2 &= \dot{x}_{s2} - \rho\dot{x}_{m2} = -a(x_{s2}) - b\sin(x_{s1}) + l\cos(x_{s1})\cdot\sin(x_{s1}) + h\cos\omega t + \Delta\xi + d(t) + u \\ &\quad - \rho[-a(x_{m2}) - b\sin(x_{m1}) + l\cos(x_{m1})\cdot\sin(x_{m1}) + h\cos\omega t] \\ &= -a(e_2) - b[\sin(x_{s1}) - \rho\sin(x_{m1})] + l[\cos(x_{s1})\cdot\sin(x_{s1}) - \rho\cos(x_{m1})\cdot\sin(x_{m1})] \\ &\quad + h[1-\rho]\cos\omega t + \Delta\xi + d(t) + u(t). \end{aligned} \tag{7}$$

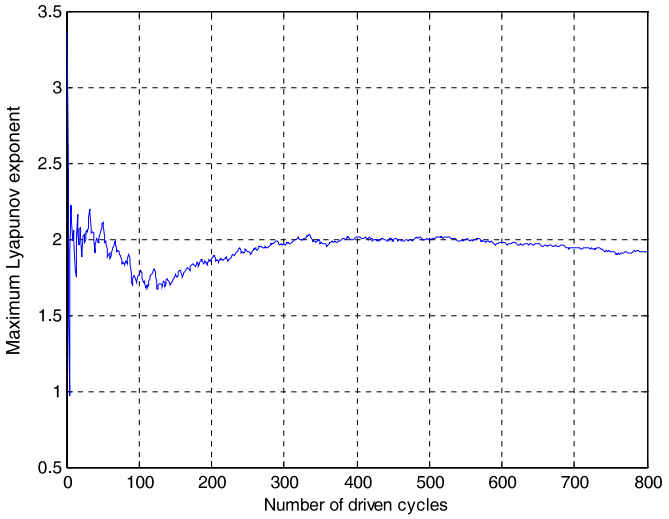

Fig. 9. Maximum Lyapunov exponent of uncertain HPS trajectory plot.

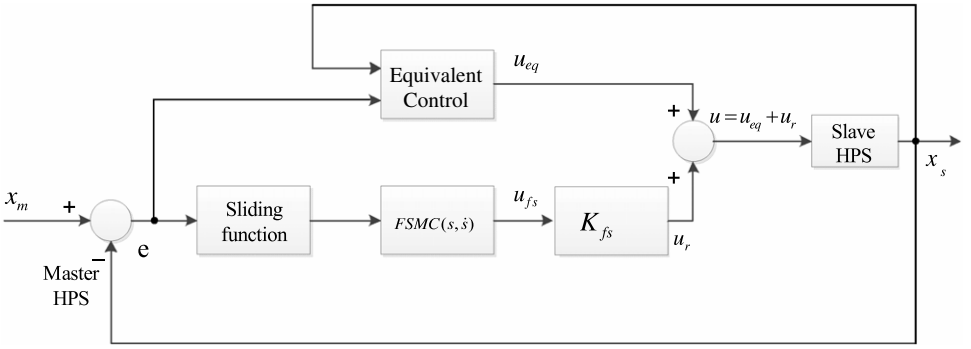

Fig. 10. Diagram of the FSMC.

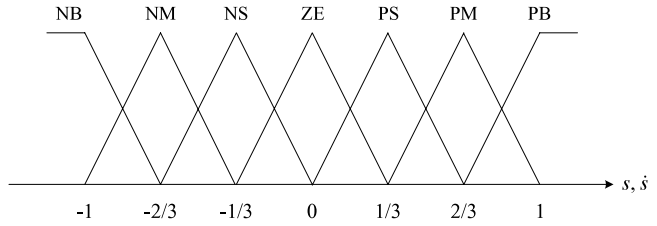

(a) Membership function of s and $\dot{s}$.

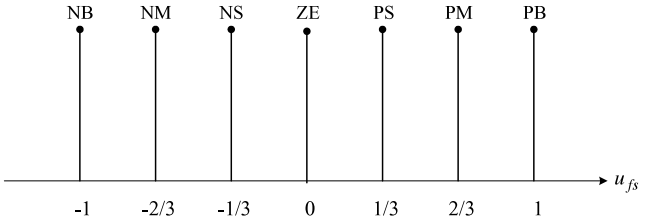

(b) Membership function of u_{fs}.

Fig. 11. Membership functions of the input–output variables for FSMC.

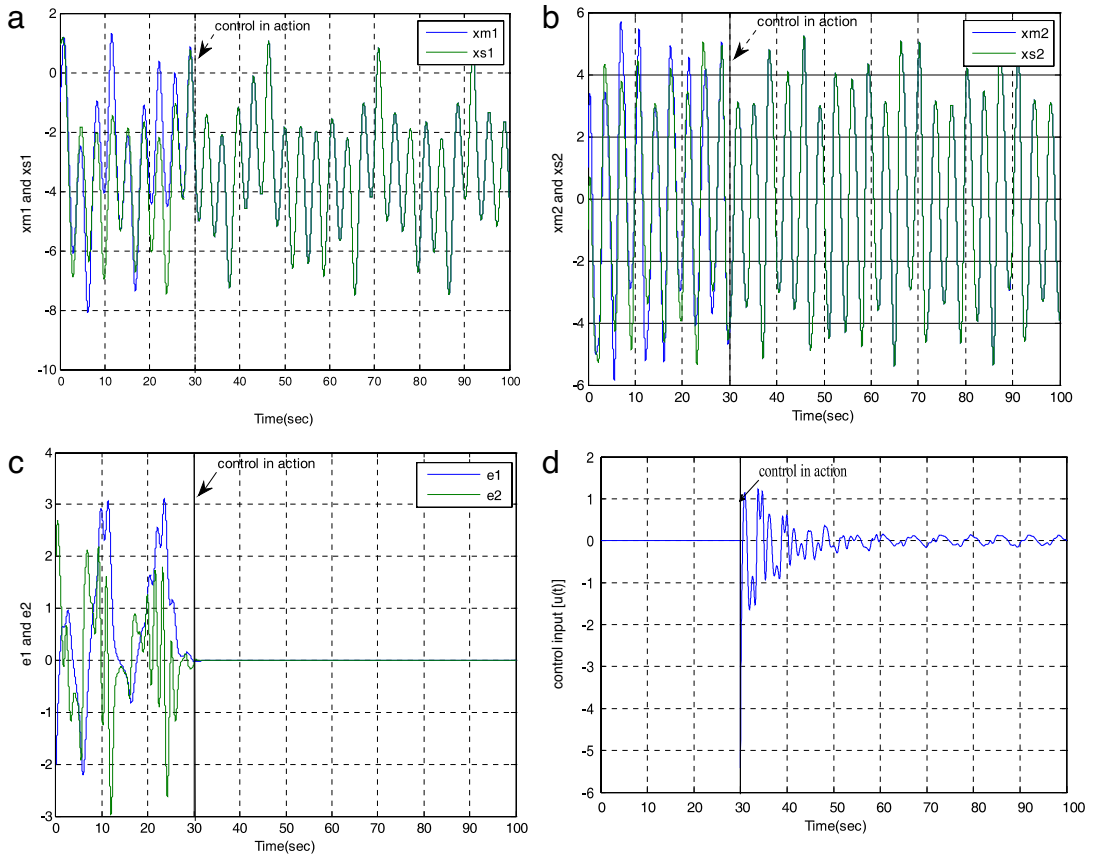

Fig. 12. Simulation results for complete synchronization $\rho = 1$ as $u(t) = 30$ is applied at 30 s: (a) x_{m1}, x_{s1} state responses; (b) x_{m2}, x_{s2} state responses; (c) error e_1, e_2 responses; (d) control signal u.

In the sliding mode control, the sliding surface chosen is defined as

$$s = c_1 e_1 + e_2 \tag{8}$$

and the close loop system then satisfies $\dot{s} = 0$.

$$\begin{aligned} \dot{s} = \; & c_1 \dot{e}_1 + \dot{e}_2 \\ \Rightarrow \; & c_1 e_2 - a(e_2) - b\,[\sin(x_{s1}) - \rho \sin(x_{m1})] + h[1-\rho]\cos\omega t \\ & + l[\cos(x_{s1}) \cdot \sin(x_{s1}) - \rho \cos(x_{m1}) \cdot \sin(x_{m1})] + \Delta\xi + d\,(t) + u_{eq} = 0. \end{aligned} \tag{9}$$

The equivalent controller u_{eq} is obtained as

$$\begin{aligned} u_{eq} = \; & -c_1 e_2 + a(e_2) + b\,[\sin(x_{s1}) - \rho \sin(x_{m1})] - l[\cos(x_{s1}) \cdot \sin(x_{s1}) - \rho \cos(x_{m1}) \cdot \sin(x_{m1})] \\ & - h[1-\rho]\cos\omega t - \Delta\xi - d\,(t)\,. \end{aligned}$$

In the real word, the system uncertainty $\Delta\xi$ and external disturbance $d(t)$ are unknown and the implemented control input is described by

$$\begin{aligned} u_{eq} = \; & -c_1 e_2 + a(e_2) + b\,[\sin(x_{s1}) - \rho \sin(x_{m1})] - h[1-\rho]\cos\omega t \\ & - l[\cos(x_{s1}) \cdot \sin(x_{s1}) - \rho \cos(x_{m1}) \cdot \sin(x_{m1})]. \end{aligned} \tag{10}$$

In the sliding mode, the error dynamics becomes

$$\dot{e}_1 = e_2 = -c_1 e_1, \tag{11a}$$

$$\dot{e}_2 = -c_1 e_2. \tag{11b}$$

Provided that the parameter c_1 is assigned a positive value, the stability of Eq. (11a) is assured, i.e. $(e_1, e_2) \to 0$ as $t \to \infty$. In other words, the slave chaotic HPS is asymptotically generalized projective synchronized to the master HPS. It is worth noting here, that the rate of convergence to the sliding surface is governed by the value assigned to parameter c_1.

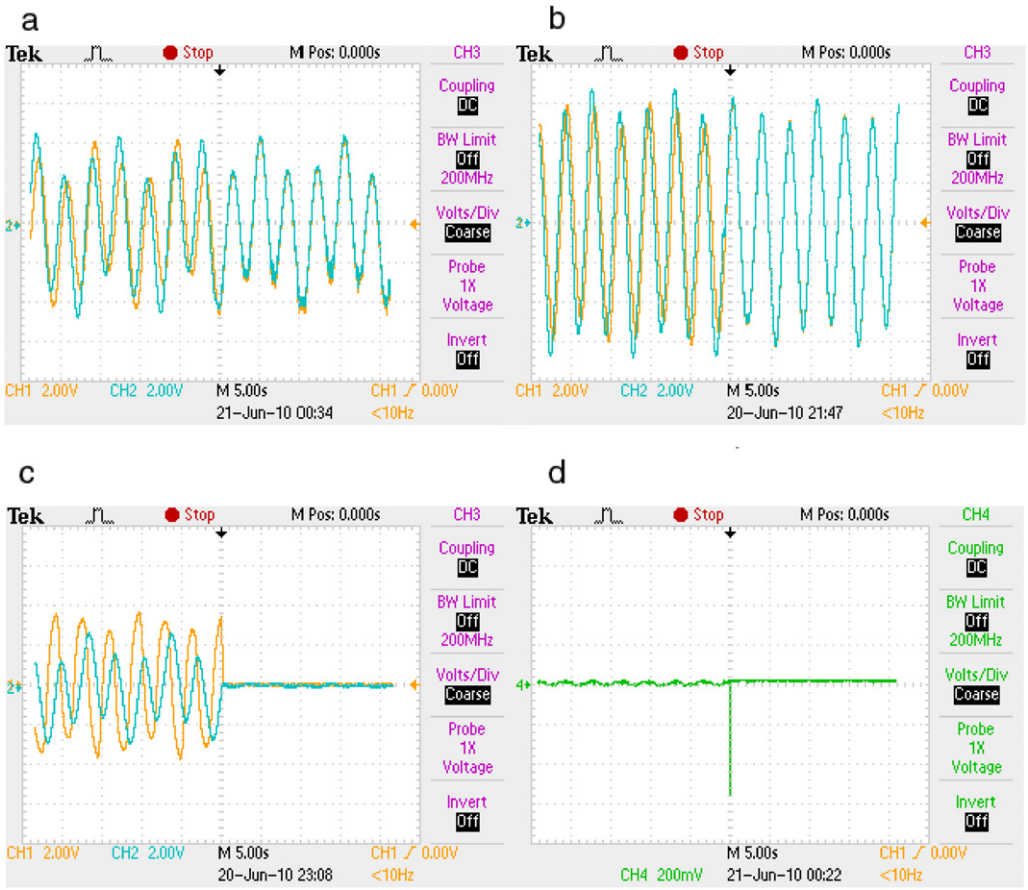

Fig. 13. Experiment results for complete synchronization $\rho = 1$: (a) x_{m1}, x_{s1} state responses; (b) x_{m2}, x_{s2} state responses; (c) error e_1, e_2 responses; (d) control signal u.

The FSMC control scheme is shown in Fig. 10; it contains an equivalent control part and a two-input–single-output FSMC. The output of the equivalent control is defined in Eq. (10), while the reaching law is given by

$$u_r = k_{fs} u_{fs}, \tag{12}$$

where k_{fs} is a normalization factor of the output variable and u_{fs} is the output of the FSMC [17], and is determined in accordance with the normalized outputs of the SMC, i.e. s and $\dot{s}$. Therefore, the overall control signal, u, has the form

$$u = u_{eq} + k_{fs} u_{fs}. \tag{13}$$

The fuzzy control rules are represented by the mapping of the input linguistic variables s and $\dot{s}$ to an output linguistic variable u_{fs}, i.e.

$$u_{fs} = FSMC(s, \dot{s}), \tag{14}$$

where $FSMC(\bullet, \bullet)$ denotes the functional characteristics of the fuzzy linguistic decision scheme. The corresponding fuzzy rule table is presented in Table 1 [11]. The membership function of input linguistic variables s and $\dot{s}$, and the membership functions of output linguistic variable u_{fs} are shown in Fig. 11, respectively. They are decomposed into seven fuzzy partitions expressed as negative big (NB), negative medium (NM), negative small (NS), zero (ZE), positive small (PS), positive medium (PB) and positive big (PB). The fuzzy rule table is designed as in Table 1 [21] and the overall control became

$$\begin{aligned} u &= u_{eq} + k_{fs} u_{fs} \\ &= -c_1 e_2 + a(e_2) + b\,[\sin(x_{s1}) - \rho \sin(x_{m1})] + k_{fs} u_{fs} \\ &\quad - l[\cos(x_{s1}) \cdot \sin(x_{s1}) - \rho \cos(x_{m1}) \cdot \sin(x_{m1})] - h[1 - \rho] \cos \omega t. \end{aligned} \tag{15}$$

In order to prove the stability of the proposed scheme (15), a Lyapunov function $V(t)$ is chosen as

$$V(t) = \frac{1}{2} s^2. \tag{16}$$

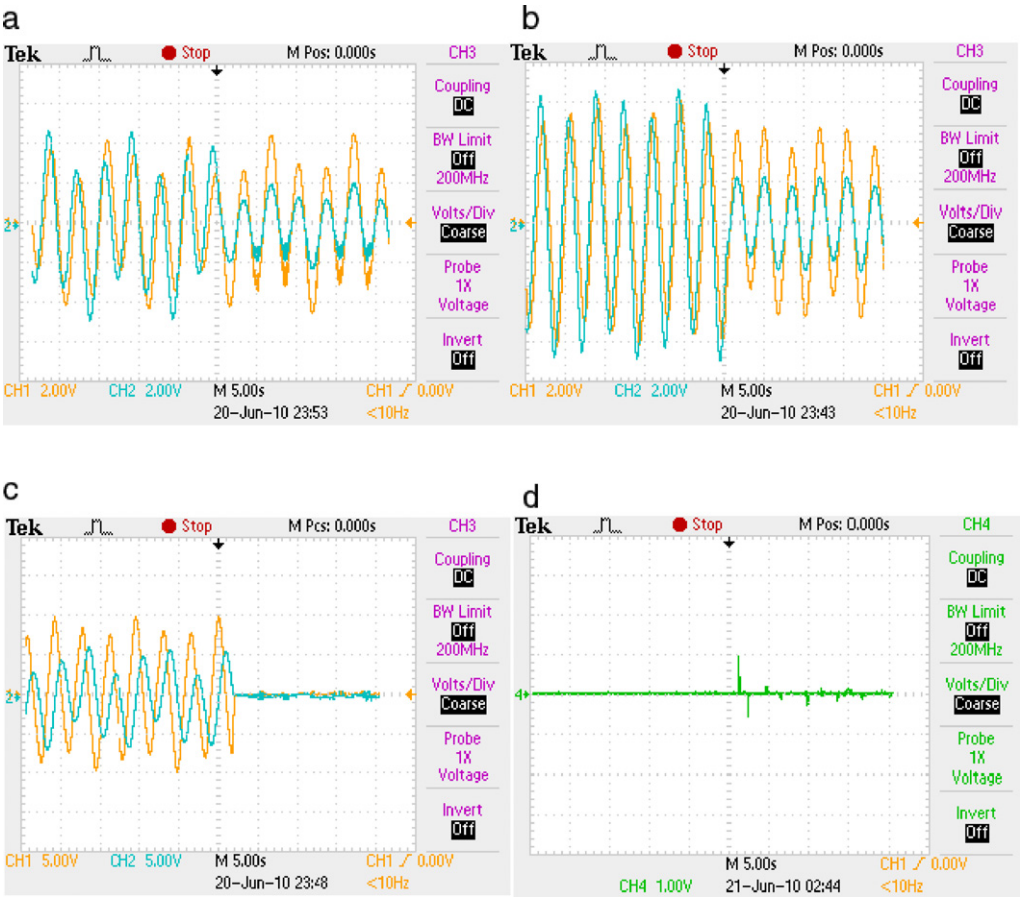

Fig. 14. Experiment results for projective synchronization $\rho = 0.5$: (a) x_{m1}, x_{s1} state responses; (b) x_{m2}, x_{s2} state responses; (c) error e_1, e_2 responses; (d) control signal u.

Substitution of Eq. (15) into Eq. (16) results in a first order derivative as

$$\begin{aligned}\dot{V} &= s\dot{s}\\ &= s\left[c_1 e_2 + \dot{e}_2\right]\\ &= s\{c_1 e_2 - a(e_2) - b[\sin(x_{s1}) - \rho\sin(x_{m1})] + l[\cos(x_{s1})\sin(x_{s1}) - \rho\cos(x_{m1})\sin(x_{m1})]\\ &\quad + h[1-\rho]\cos\omega t + \Delta\xi + d(t) + u_{eq} + k_{fs}u_{fs}\}\\ &= s\left[\Delta\xi + d(t) + k_{fs}u_{fs}\right]. \end{aligned} \tag{17}$$

Assuming that $|\Delta\xi| \le \gamma$, $|d(t)| \le \delta$ are bounded, it then follows that

$$\begin{aligned}\dot{V} &\le |s|\cdot[|\Delta\xi| + |d(t)|] - k_{fs}\cdot|s|\\ &\le |s|\cdot\left(\gamma + \delta - k_{fs}\right) = -\left(k_{fs} - (\gamma+\delta)\right)|s|. \end{aligned} \tag{18}$$

The system stability is assured on a condition $k_{fs} > (\gamma + \delta)$ such that $\dot{V} < 0$. It guarantees the robust stability of the control law (15), and the master–slave system achieves global GPS.

4. Numerical simulation and experimental results

This section performs numerical simulations and experiments to demonstrate the feasibility and effectiveness of the proposed FSMC scheme in generalized projective chaos synchronization controlling of master–slave HPS. Eqs. (3), (4) and (15) are simulated in the context of fuzzy sliding synchronization, and experiment on the implemented hardware is carried out as follows. Setting the parameters $c_1 = 10, W = 1, \Delta\zeta = 0.1\sin(t)$ and $d(t) = 0.1\cos(t)$ satisfy, respectively $|\Delta\zeta| \le \gamma = 0.1$ and $|d(t)| \le \delta = 0.1$. The initial conditions are defined as $x_1(0) = 0$ and $x_2(0) = 0$. As demonstrated in Fig. 12, the complete synchronization ($\rho = 1$) between the master and the slave systems is not reached until the control is in action. Shown in Fig. 13 is the time response in the implemented hardware chaos synchronization system. The control

Table 1
Fuzzy rule table.

u \ s / ṡ	NB	NM	NS	ZE	PS	PM	PB
PB	NB	NB	NB	NB	NM	NS	ZE
PM	NB	NB	NB	NM	NS	ZE	PS
PS	NB	NB	NM	NS	ZE	PS	PM
ZE	NB	NM	NS	ZE	PS	PM	PB
NS	NM	NS	ZE	PS	PM	PB	PB
NM	NS	ZE	PS	PM	PB	PB	PB
NB	ZE	PS	PM	PB	PB	PB	PB

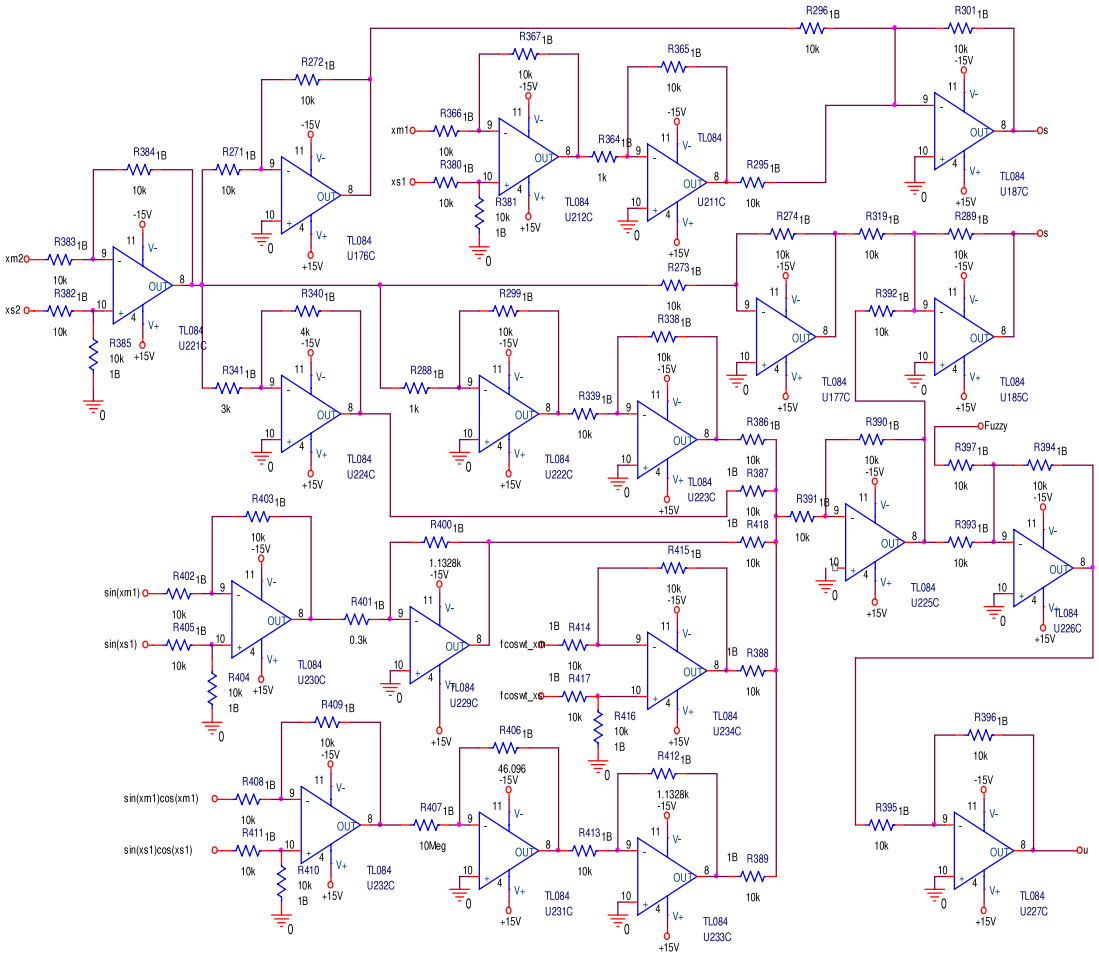

Fig. 15. Circuit diagram of fuzzy sliding mode controller implemented in ORCAD.

is in action at the middle point of the time axis, for the reason that there is no way to activate the controller precisely at the specified time point. These results show a convergence to a very small synchronization error. The experimental results of projective synchronization for $\rho = 0.5$ are shown in Fig. 14. The results also show that the projective synchronization can be reached by the same control scheme. Shown in Figs. 15 and 16 are the circuitry and the entity photo of such a fuzzy sliding mode controller respectively.

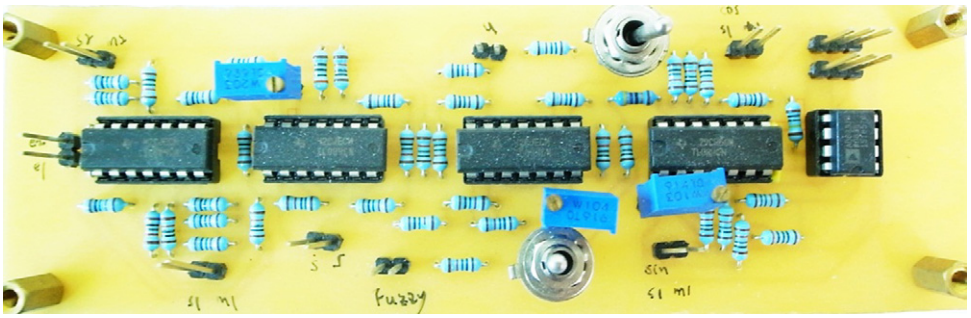

Fig. 16. Photo of fuzzy sliding mode controller circuit module.

5. Conclusion

This paper presents a controller operating in the fuzzy sliding mode such that the state responses of the master and slave systems alike are thus GPS in the context of parameter variation and external disturbance. Taking into account the external disturbance and tolerance in electronic components in the hardware aspect, the robustness is a concern essential to the design of the controller, leading to the choice of fuzzy sliding control. Owing to the fact that the sign function, utilized in the sliding mode control, results in server chattering at a high switching rate, a controller is made fuzzy as a way to remove such chattering problems. Sending s, $\dot{s}$ to the controller, the sliding function s is thus enabled to converge to zero, within a short period of time, by the use of a knowledge base, according to which the decision is made. As such, it is concluded, by either simulation or experiment, that the fuzzy sliding controller demonstrates the combined advantages of a sliding and a fuzzy controller, thereby reducing the chattering problem significantly.

Acknowledgment

The financial support provided to this study by the National Science Council of the R.O.C. under Grant No. NSC-100-2221-E-167-004 is greatly appreciated.

References

[1] E.N. Lorenz, Deterministic non-periodic flow, J. Atmospheric Sci. 20 (1963) 130–141.
[2] G. Duffing, Erzwungene Schwingungen bei veränderlicher Eigenfrequenz und ihre technische Bedeutung, Friedr. Vieweg u. Sohn, Braunschweig, 1918.
[3] O. Rössler, An equation for continuous chaos, Phys. Lett. A 57 (1976) 397–398.
[4] L.O. Chua, G.N. Lin, Canonical realization of Chua's circuit family, IEEE Trans. Circuit Syst. 37 (7) (1990) 885–902.
[5] Z.M. Ge, T.C. Yu, Y.S. Chen, Chaos synchronization of a horizontal platform system, J. Sound Vib. 268 (4) (2003) 731–749.
[6] Z.F. Wu, J.P. Cai, M.H. Wang, Master–slave chaos synchronization criteria for the horizontal platform systems via linear state error feedback control, J. Sound Vib. 295 (2006) 378–387.
[7] Z.F. Wu, J.P. Cai, M.H. Wang, Robust synchronization of chaotic horizontal platform systems with phase difference, J. Sound Vib. 305 (2006) 481–491.
[8] M. Mihua, C. Jianping, L. Meili, Robust synchronization with error bound of horizontal platform systems with parameter mismatch, in: Proc. IEEE. 27th Chinese Control Conf., 2008, pp. 302–306.
[9] E. Ott, C. Grebogi, J.A. Yorke, Controlling chaos, Phys. Rev. Lett. 64 (1990) 1196–1199.
[10] L.M. Pecora, T.L. Carroll, Synchronization in chaotic systems, Phys. Rev. Lett. 64 (1990) 821–824.
[11] S. Mascolo, G. Grassi, Controlling chaotic dynamics using backstepping design with application to the Lorenz system and Chua's circuit, Int. J. Bifur. Chaos 9 (1999) 1425–1434.
[12] G. Chen, X. Dong, From Chaos to Order: Methodologies, Perspectives and Applications, World Scientific, Singapore, 1998.
[13] S. Chen, J. Lü, Synchronization of an uncertain unified chaotic system via adaptive control, Chaos Solitons Fractals 14 (2002) 643–647.
[14] S. Dadras, H.R. Momeni, Adaptive sliding mode control of chaotic dynamical systems with application to synchronization, Math. Comput. Simul. 80 (2010) 2245–2257.
[15] M. Roopaei, M.Z. Jahromi, R. John, T.C. Lin, Unknown nonlinear chaotic gyros synchronization using adaptive fuzzy sliding mode control with unknown dead-zone input, Commun. Nonlinear Sci. Numer. Simul. 15 (2010) 2536–2545.
[16] A. Poursamad, A.H.D. Markazi, Adaptive fuzzy sliding-mode control for multi-input multi-output chaotic systems, Chaos Solitons Fractals 42 (2009) 3100–3109.
[17] H.T. Yau, C.C. Wang, C.T. Hsieh, C.C. Cho, Nonlinear analysis and control of the uncertain micro-electro–mechanical system by using a fuzzy sliding mode control design, SCI Comput. Math. Appl. 61 (8) (2011) 1912–1916.
[18] S.J. Wang, N.S. Pai, H.T. Yau, Robust controller design for synchronization of two chaotic circuits, Inf. Technol. J. 8 (5) (2009) 743–749.
[19] R. Mainieri, J. Rehacek, Projective synchronization in the three-dimensional chaotic systems, Phys. Rev. Lett. 82 (15) (1999) 042–3045.
[20] C.L. Kuo, Design of an adaptive fuzzy sliding-mode controller for chaos synchronization, Int. J. Nonlinear Sci. Numer. Simul. 8 (4) (2007) 631–636.
[21] C.L. Kuo, H.T. Yau, Y.C. Pu, Design and implement of a digital PID controller for a chaos synchronization system by evolutionary programming, J. Appl. Sci. 8 (3) (2008) 2420–2427.
[22] S. Haykin, X.B. Li, Detection of signals in chaos, Proc. IEEE 83 (1) (1995) 95–122.